EUROPEAN RESPIRATORY journal

FLAGSHIP SCIENTIFIC JOURNAL OF ERS

Early View

Original research article

Mechanical ventilation promotes lung tumor spread by modulation of cholesterol cell content

Inés López-Alonso, Cecilia López-Martínez, Paula Martín-Vicente, Laura Amado-Rodríguez, Adrián González-López, Juan Mayordomo-Colunga, Cecilia del Busto, Marina Bernal, Irene Crespo, Aurora Astudillo, Miguel Arias-Guillén, Antonio Fueyo, Isaac Almendros, Jorge Otero, Héctor Sanz-Fraile, Ramón Farré, Guillermo M Albaiceta

Please cite this article as: López-Alonso Iés, López-Martínez C, Martín-Vicente P, *et al*. Mechanical ventilation promotes lung tumor spread by modulation of cholesterol cell content. *Eur Respir J* 2021; in press (https://doi.org/10.1183/13993003.01470-2021).

Mechanical ventilation promotes lung tumor spread by modulation of cholesterol cell content

Inés López-Alonso[1,2,3,#,*], Cecilia López-Martínez[1,2#], Paula Martín-Vicente[1,2], Laura Amado-Rodríguez[1,2,3,4], Adrián González-López[1,5], Juan Mayordomo-Colunga[1,2,6], Cecilia del Busto[2,7], Marina Bernal[8], Irene Crespo[9], Aurora Astudillo[2], Miguel Arias-Guillén[1,2,10], Antonio Fueyo[3,9,11], Isaac Almendros[1,12,13], Jorge Otero[1,12], Héctor Sanz-Fraile[12], Ramón Farré[1,12,13], Guillermo M Albaiceta[1,2,3,4,9].

[1]Centro de Investigación Biomédica en Red-Enfermedades Respiratorias. Madrid. Spain. [2]Instituto de Investigación Sanitaria del Principado de Asturias. Oviedo, Spain. [3]Instituto Universitario de Oncología del Principado de Asturias. Oviedo, Spain. [4]Unidad de Cuidados Intensivos Cardiológicos. Hospital Universitario Central de Asturias. Oviedo, Spain. [5]Department of Anesthesiology and Operative Intensive Care Medicine CCM/CVK, Charité - Universitätsmedizin Berlin, Germany. [6]Unidad de Cuidados Intensivos Pediátricos. Hospital Universitario Central de Asturias. Oviedo, Spain. [7]Unidad de Cuidados Intensivos Polivalente. Hospital Universitario Central de Asturias. Oviedo, Spain. [8]Servicio de Medicina Interna. Fundación Jiménez Díaz. Madrid-Spain. [9]Departamento de Biología Funcional. Universidad de Oviedo. Oviedo, Spain. [10]Servicio de Neumología. Hospital Unviersitario Central de Asturias. Oviedo, Spain. [11]Centro de Investigación Biomédica en Red-Oncología. Madrid, Spain. [12]Unitat Biofísica i Bioenginyeria, Facultat de Medicina i Ciències de la Salut, Universitat de Barcelona, Barcelona, Spain. [13]Institut Investigacions Biomèdiques August Pi Sunyer, Barcelona, Spain.

[#]These authors contributed equally.

[*]**Corresponding author:**

Inés López-Alonso

Instituto de Investigación Sanitaria del Principado de Asturias

Avenida del Hospital Universitario s/n

33011 Oviedo. Spain

E-mail: ila@crit-lab.org

Author contributions

Study design: ILA, GMA, LAR. Cell and animal studies: ILA, CLM, PMV, IC, AF, AA. RNA sequencing analysis: CLM, AGL, GMA. Cell stretch and Atomic Force Microscopy: IA, HSF, JO, RF. Clinical study: JMC, CdB, MB, MAG, LAR, GMA. Data analysis: ILA, CLM, GMA. Manuscript writing: ILA, GMA. Manuscript review and editing: All authors.

Financial support

Funded by Centro de Investigación Biomédica en Red (CIBER)-Enfermedades Respiratorias (Madrid, Spain, grant CB17/06/0021), Instituto de Salud Carlos III (Madrid, Spain, grants PI13/02189, PI16/01614 and PI20/01360) and Asociación Española Contra el Cancer (PPLVE18060). Instituto Universitario de Oncología del Principado de Asturias is supported by Fundación Liberbank. ILA was the recipient of a grant from Ministerio de Ciencia, Innovación y Universidades, Spanish Government (CAS19/00209). CLM is the recipient of a grant from Ministerio de Universidades, Spain (FPU18/02965). LAR was

the recipient of a grant from Instituto de Salud Carlos III, Spain (CM16/00128) and a mobility grant from CIBERES, Instituto de Salud Carlos III, Spain.

Take-home message: Even a short course of mechanical ventilation, such as during major surgery, promotes lung cancer dissemination. A mechano-dependent modulation of cholesterol intake regulates cancer cell stiffness and could be a new therapeutic target in this setting.

Abstract

Mechanical stretch of cancer cells can alter their invasiveness. During mechanical ventilation, lungs may be exposed to an increased amount of stretch, but the consequences on lung tumors have not been explored.

To characterize the influence of mechanical ventilation on the behavior of lung tumors, invasiveness assays and transcriptomic analyses were performed in cancer cell lines cultured in static conditions or under cyclic stretch. Mice harbouring lung melanoma implants were submitted to mechanical ventilation and metastatic spread was assessed. Additional *in vivo* experiments were performed to determine the mechano-dependent specificity of the response. Incidence of metastases was studied in a cohort of lung cancer patients that received mechanical ventilation compared with a matched group of non-ventilated patients.

Stretch increases invasiveness in melanoma B16F10luc2 and lung adenocarcinoma A549 cells. We identified a mechanosensitive upregulation of pathways involved in cholesterol processing *in vitro*, leading to an increase in PCSK9 and LDLR expression, a decrease in intracellular cholesterol and preservation of cell stiffness. A course of mechanical ventilation in mice harboring melanoma implants increased brain and kidney metastases two weeks later. Blockade of PCSK9 using a monoclonal antibody increased cell cholesterol and stiffness and decreased cell invasiveness *in vitro* and metastasis *in vivo*. In patients, mechanical ventilation increased PCSK9 abundance in lung tumors and the incidence of metastasis, thus decreasing survival.

Our results suggest that mechanical stretch promote invasiveness of cancer cells, which may have clinically relevant consequences. Pharmacological manipulation of cholesterol endocytosis could be a novel therapeutic target in this setting.

Keywords: Lung cancer; Metastasis; Cholesterol intake; PCSK9

Introduction

Mechanical stretch can alter cell behavior. Once a force is applied on the cell surface, it is transduced into a large variety of biological responses (1). Several cell structures, from stretch-activated ion channels in plasma membrane to the nuclear envelope itself act as mechanosensors (2). The triggered responses are also variable, depending on the cell lineage and the stimulus, and may include differentiation (3), apoptosis (4), secretion of molecules (5) or activation of the inflammatory response (6) among others.

The respiratory system is subjected to a mechanical load in every breath. In healthy lungs during spontaneous breathing, the magnitude of the applied forces is low and evenly distributed along a homogeneous parenchyma. However, these forces can be increased in several conditions. During conventional mechanical ventilation, lung tissue can be exposed to high positive pressures. Moreover, in a heterogeneous lung, forces are amplified, especially at the air-tissue interfaces. This increased mechanical load is responsible for the so-called ventilator-induced lung injury (VILI) (7). This syndrome is characterized by the activation of a proinflammatory response within the lungs, with epithelial apoptosis and extracellular matrix remodeling. Recently, we have shown that mechanical ventilation modifies the nuclear envelope (8), activating p53-dependent pathways and causing epithelial cell reprogramming (9).

Lung neoplasms, either primary or metastatic, are relatively common. Primary lung cancer accounts for 11.6% or total cancer cases (2.09 million new cases in 2018) (10) and 20-54% of malignant tumors have pulmonary metastases (11, 12). These neoplastic

cells are exposed to mechanical forces during the normal respiratory cycle, but especially if positive pressures are applied. Apart from other causes, up to 40% of the lung cancer patients require resection surgery (13) and, thus, mechanical ventilation. The intra-alveolar positive pressure applied during mechanical ventilation and the changes in lung architecture caused by the tumor may increase air-tissue and air-tumor interfaces, amplifying the forces supported by the cells (14). Cancer cells are mechanosensitive. Different mechanical stimuli such as solid stress, fluid pressure or changes in stiffness or environment microarchitecture have been described as drivers of tumor progression in experimental models (15, 16). However, the consequences of the resulting mechanotransduction during mechanical ventilation on these processes have not been explored.

It has been described that substrate rigidity modulates cell cholesterol content (17), which in turn determines membrane stiffness. Soft membranes facilitate cell motility and migration (18), making cholesterol metabolism a key mechanism in cancer cell invasiveness (19). Proprotein convertase subtilisin/kexin type 9 (PCSK9) is an enzyme involved in LDLR turnover and a major regulation of cell cholesterol intake.

The objective of this work is to characterize the influence of mechanical ventilation on the behavior of lung tumors. We hypothesized that mechanical stretch would result in a more aggressive phenotype of cancer cells, both *in vitro* and *in vivo*. To test this hypothesis and identify the underlying mechanisms, we studied cancer cells *in vitro* and *in vivo* models of lung cancer and metastasis. Our results support the hypothesis and point to novel therapeutic targets that could help to improve the outcome of cancer patients submitted to mechanical ventilation.

Methods

To test the hypothesis that the cyclic stretch of mechanical ventilation increases cancer cell aggressiveness, a combination of cell and animal experiments and clinical observations were performed. A detailed description of the methods can be found in the online supplement.

Cell culture experiments. Mouse melanoma B16F10luc2 and human lung adenocarcinoma A549 cells were cultured in static conditions or stretched (15% elongation, 15 cycles/min) for 24 hours, and their invasiveness studied in Matrigel transwells. In order to study the possible effect of paracrine factors, cells and supernatants were combined, resulting in 4 experimental groups (static cells + static supernatant; static cells + stretched supernatant; stretched cells + static supernatant; stretched cells + stretched supernatant). Fibrillar and globular actin were stained, and cell stiffness measured using atomic force microscopy. In addition, RNA was extracted and sequenced using standard protocols. Differentially expressed genes were confirmed by quantitative PCR and analyzed using the Ingenuity Pathways Analysis tool. In confirmatory experiments, cells were cultured with different concentrations of cholesterol, an increased CO_2 concentration or treated with a PCSK9 inhibitor (alirocumab) or an unspecific human IgG.

Animal model. The protocol was approved by the Animal Research Committee at Universidad de Oviedo. Anesthetized mice were injected with 15000 B16F10luc2 cells and left to recover for 15 days. Then, were anesthetized again and submitted to a 2-hour period of mechanical ventilation (peak inspiratory pressure 15 cmH_2O, PEEP 2 cmH_2O, 100 breaths/min) or spontaneous breathing, and sacrificed immediately or after 15 additional days. Brain, lungs and kidneys were harvested and processed for

histological studies, cholesterol measurements and quantitative PCR. Additional series using animals with liver metastases (via spleen injection) or treated with LPS instead of mechanical ventilation were added to exclude other mechanisms involved in cancer progression. Finally, mice with lung melanoma implants were treated with three doses of alirocumab or unspecific IgG before mechanical ventilation, and followed for 15 days as previously described, to study the impact of the treatment on the metastatic spread promoted by ventilation.

Clinical study. This retrospective study was approved by the regional clinical research ethics committee. In 6 patients with lung adenocarcinoma, PCSK9 immunofluorescence was performed in paired samples obtained by percutaneous large-bore needle aspiration (under spontaneous breathing) and after surgical resection of the tumor (after mechanical ventilation). In addition, a group of consecutive patients (n=28) with lung cancer without distant metastases who received mechanical ventilation by any cause other than lung cancer resection were matched by age, sex and cancer stage to a group of patients (n=58) who were not mechanically ventilated. To characterize the effect of mechanical ventilation on the development of metastases in patients, a multi-state Markov model was fitted, and survival and probability of developing metastasis over time calculated.

Statistical analysis. Results were compared among groups using an ANOVA (for more than 2 experimental groups) or a Wilcoxon test (for two groups). Categorical variables were compared using a chi-square test. Two-sided P-values were calculated. Details on RNA-seq analysis and the Markov model used in patients' follow-up can be found in the online supplement.

Results

Mechanical stretch increases cancer cell invasiveness

B16F10luc2 melanoma cells seeded in silicon plates were cultured in static conditions or submitted to cyclic mechanical stretch (15% surface elongation, 15 cycles/min) for 24 hours (Figure 1A). Stretched cells showed an increase in fibrillar actin, a marker of an increased mechanical load (Supplementary figure 1). After this time, supernatants were collected and cells removed, washed, resuspended in the collected supernatants and seeded in Matrigel chambers to study invasion. Supernatants and cells were combined to cover the four possible combinations of static/stretched cells and supernatants. After 24 additional hours, cell migration was assessed. Stretched cells showed an increased invasiveness compared to their counterparts cultured in static conditions, irrespective of supernatant conditioning (Figure 1B-C).

To identify the mechanisms triggered by stretch and responsible for this increase in invasiveness, RNA from B16F10luc2 cells cultured under cyclic stretch or static conditions was extracted, purified and sequenced, and differential gene expression assessed. Stretch induced a massive cell reprogramming, with significant differences in the expression of 5847 genes (Figure 1D). Pathway enrichment using Ingenuity Pathway Analysis revealed a significant overexpression of several molecular routes involved in cancer pathogenesis (Figure 1E). Interestingly, cholesterol-related pathways were the top ranked molecular networks among the differentially expressed genes, and a specific molecular network was identified (Figure 1F). The increased expression of *Pcsk9* and *Ldlr* in response to stretch were confirmed using quantitative PCR (Figure 1G-H). In line with these findings, intracellular cholesterol levels decreased after mechanical stretch (Figure

1I). PCSK9 was selected as potential therapeutic target, as there are commercially available inhibitors.

Intracellular cholesterol depletion is needed for stretch-induced invasiveness

We then explored the effect of the manipulation of intracellular cholesterol levels on the invasiveness of cancer cells. B16F10luc2 melanoma cells were cultured in lipid-depleted medium and standard FBS with different cholesterol concentrations (Figure 2A). Lipid depletion increased the invasiveness of B16F10luc2 cells. However, cholesterol supplementation did not exert a significant effect.

The effects of PCSK9 inhibition in stretch-induced invasiveness were assessed. B16F10luc2 cells were cultured, treated with alirocumab, a monoclonal antibody against PCSK9, or unspecific IgG for 3 days, and submitted to mechanical stretch. Alirocumab decreased cell invasion after stretch (Figure 2B) and increased intracellular cholesterol levels (Figure 2C). Interestingly, the combination of alirocumab and mechanical stretch significantly increased nuclear envelope stiffness, measured using atomic force microscopy (Figure 2D).

To extend the validity of these findings, key experiments were repeated in A549 lung adenocarcinoma cells. In this cell line, mechanical stretch increased their invasiveness, there was an increase in *PCSK9* expression and treatment with alirocumab ameliorated their invasive potential (Figure 3A-C).

Collectively, these results suggest that mechanical stretch increases cell invasiveness, and that blockade of cholesterol intake interferes with this invasive phenotype, possibly by increasing membrane stiffness.

Mechanical ventilation promotes metastasis in an animal model of lung melanoma

To translate these findings and gain further insight of the therapeutic potential of PCSK9 inhibition in this setting, we developed an animal model of lung tumors and mechanical stretch (Figure 4A). B16F10luc2 melanoma cells were injected via jugular vein in 8-week-old male mice. After two weeks, these mice had lung metastases, demonstrated after luciferin injection and histology preparations (Figure 4B). At this time point, these animals and their medium-injected counterparts were randomized to receive mechanical ventilation (120 minutes, peak inspiratory pressure 15 cmH_2O, PEEP 2 cmH_2O, 100 breaths/min) or a sham procedure (spontaneous breathing under sedation for 120 minutes). Animals with and without cancer cells and sacrificed immediately after ventilation showed an increase in fibrillar actin (Supplementary Figure 2) with no significant differences in lung damage (Figure 4C-D). Quantification of PCSK9 in immunohistochemical sections revealed a significant increase in both normal and tumor tissue (Figure 4E-F).

Additional animals were followed up for two weeks after ventilation, and then anesthetized and brain and kidneys harvested. Micrometastases were identified by detection of luciferase expression by quantitative PCR, and a metastasis score was quantified as the proportion of positive samples. No brain or kidney metastases were detected by qPCR in any animal sacrificed immediately after ventilation. However, mechanical ventilation increased the incidence of metastases two weeks after ventilation (Figure 4G), in line with the effects observed after cell stretch. In a separate series, tumor-harboring mice were treated with alirocumab or unspecific IgG and mechanically ventilated as previously described. Alirocumab decreased the incidence of metastases (Figure 4H). Brain sections stained with antibodies against GP100, a specific

melanoma marker, revealed positive cells only in samples from animals with positive detection by PCR, confirming the accuracy of the technique (Supplementary Figure 3).

Mechanical ventilation may cause local and systemic inflammation that could facilitate the systemic spread of tumor cells. To characterize the relevance of these effects, three different experiments were carried out. First, mice with liver tumors (caused by injection of B16F10luc2 cells in the spleen, followed by splenectomy) were submitted to an identical protocol. Mechanical ventilation did not increase the incidence of lung or kidney metastases in these animals (Supplementary figure 4A). Second, mice with lung metastases were treated with LPS or saline two weeks after cell injection, followed for two additional weeks, and the organs harvested. Again, no differences in the incidence of metastases were observed (Supplementary figure 4B). Finally, to discard that a potential anti-metastatic effect of hypercapnia in the anesthetized, non-ventilated group, B16F10 cells were cultured in presence of 5 and 20% CO_2. Carbon dioxide increased, rather than decreased cell invasiveness (Supplementary Figure 5), thus discarding an anti-metastatic effect of hypercapnia. Collectively, these results suggest that mechanical ventilation *per se* promotes metastatic spread of lung tumors by a local, inflammation-independent effect.

Mechanical ventilation increases tumor PCSK9 and accelerates metastatic spread in patients

Finally, we explored the relevance of these mechanisms in patients with lung cancer. First, we confirmed the changes in PCSK9 in response to mechanical ventilation. Immunostaining of PCSK9 was quantified in large-bore needle biopsies (thus obtained during spontaneous breathing) and in surgical resection pieces (under mechanical

ventilation) from the same patients (Figure 5A). Samples obtained under positive-pressure ventilation showed a significant increase in PCSK9 staining (Figure 5B), resembling the previous results from preclinical models.

To characterize the impact of mechanical ventilation in the outcome of lung cancer patients, 28 patients with non-metastatic, primary lung cancer, who received mechanical ventilation for any reason other than lung resection were retrospectively compared to 58 controls, matched by age, sex and tumor stage, without history of mechanical ventilation. Median age was 69 (95% confidence interval 61-72) years. Median follow-up time was 1081 days (95% confidence interval 519-2166). Univariate comparisons between these two groups are shown in Supplementary table 2. As expected, there were no differences in age, sex, comorbidities, tumor stage or risk factors between those with and without an episode of mechanical ventilation.

The course of the disease was modelled using a multi-state Markov model and the 1-year transition probabilities for each stage were computed (Figure 5C). The transition probability to a metastatic state was higher after receiving mechanical ventilation (Figure 5D) compared to the transition to metastases without mechanical ventilation, with a hazard ratio of 4.91 (2.68-9.03). Estimated survival curves from each stage are shown in Figure 5E. Compared to predicted survival after diagnosis, both mechanical ventilation (HR 1.5 [1.44-1.58] and a metastatic state (HR 3.14 [2.95-3.33]) decreased survival probabilities over time.

Discussion

Our results show that mechanical stretch enhances invasiveness of lung cancer cells. Increases in PCSK9 and LDLR expression in response to stretch result in intracellular cholesterol depletion that contributes to the preservation of the low cell stiffness required for migration. Blockade of the stretch-induced increase in PCSK9 attenuated the intracellular changes in cholesterol, increasing cell stiffness and ameliorating the increase in invasiveness in cell and animal models. Moreover, this effect may be relevant in patients with lung cancer exposed to an increased mechanical load during mechanical ventilation, such as during major surgery. Collectively, these results suggest that mechanosensing of lung cancer cells may be a clinically relevant pathogenetic mechanism and a potential therapeutic target.

The cancer cell mechanosensitive machinery that allows them to respond to applied forces include cell-ECM and cell-cell adhesions, stretch sensitive channels and the nucleus, whose downstream effectors regulate pathways involved in cell proliferation, survival, motility or metabolism (20). It has been described that an increase in tumor microenvironment stiffness is related to tumor progression(21). Cancer cells transduce these mechanical signals through a structural scaffold within the cytoplasm until reaching the nucleus. The observed increase in fibrillar actin after mechanical stretch is a marker of this increased mechanical load (22). Ultimately, these signals activate the transcription of pro-tumorigenic programs (23). Moreover, it has been shown that nuclear stiffness regulates cytoskeletal mechanics of cancer cells, thus regulating their migration and invasiveness (24, 25).

In our model, mechanical stretch was related to the activation of several pro-metastatic pathways, including triggering the unfolded protein response (26), geranylgeranyl diphosphate biosynthesis (27) or activation of the mevalonate pathway (28). Interestingly, the most over-represented routes, related to cholesterol biosynthesis and metabolism, are not canonical pro-metastatic mechanisms. Cancer cell migration requires not only an invasive phenotype, but also an increased deformability required for migration (29). Cholesterol is a major determinant of the stiffness of cell membranes. LDLR is responsible for cholesterol intake. When PCSK9 binds LDLR, the resulting complex is internalized and digested, decreasing LDLR recycling and cholesterol intake. These low intracellular cholesterol levels preserve cell stiffness and facilitate migration (17). Inhibition of PCSK9 results in internalization of LDL-LDLR complex and receptor recycling (30), thus increasing intracellular cholesterol. Cholesterol content in cell membranes increases their stiffness and impairs cell migration (31) of stretch-primed cells.

Our results show that increasing intracellular cholesterol failed to decrease cancer cell migration in absence of an additional stimulus. However, cholesterol depletion facilitated their invasiveness. Therefore, the increase in PCSK9 in response to stretch should be understood as a compensatory mechanism aimed to decrease intracellular cholesterol, thus ameliorating the stretch-related increase in cell stiffness. PCSK9 inhibition disrupts this mechanism, increasing cell stiffness and impairing migration. As there are commercially available PCSK9 inhibitors (approved as treatment for hypercholesterolemia), with a good safety profile, this convertase could be an interesting therapeutic target.

Other authors have described additional roles of PCSK9 in cancer. PCSK9 can *per se* modulate endoplasmic reticulum stress and apoptosis of neoplastic cells (32, 33). However, immunization against PCSK9 did not modify melanoma growth (34). Recently, it has been shown that PCSK9 inhibition may enhance immune checkpoint therapies for cancer (35). Our effects relating mechanical stretch, PCSK9 and invasiveness are however, independent of these findings, as no inflammatory response or additional immune regulation were present in cell cultures and no differences in lung inflammation were observed in the animal model.

Mechanical ventilation can induce both a local and systemic response to positive pressures within lung parenchyma (7). Mechanical ventilation can facilitate the engraftment of cancer cells after intravenous injection (36). However, a clinical trial comparing spontaneous breathing or mechanical ventilation during breast tumor surgery failed to demonstrate differences in long-term recurrences (37). Our models of extrapulmonary melanoma also failed to demonstrate any effect of mechanical ventilation on their metastatic spread. Rather, our results are compatible with a direct mechanical effect of positive-pressure ventilation over cancer cells. However, the impact of specific ventilatory modes or settings cannot be extrapolated from our model.

There are several clinical scenarios in which patients harboring lung tumors may be exposed to an increased mechanical load in the respiratory system. First, patients with obstructive sleep apnea may experience large intrathoracic pressure swings during airway obstruction or the use of positive pressure ventilation. These patients show an increased risk of metastatic tumors (38), which has been related to the effects of intermittent hypoxia (39) and immune dysregulation (40, 41). The contribution of this mechanical effect to the worse outcome in this population is unknown. Second, patients

with lung cancer may receive mechanical ventilation during surgery. Pneumectomy (under mechanical ventilation) is one of the main curative strategies for lung cancer, and although cancer cell may be primed by positive pressure ventilation, their immediate resection precludes further consequences. Therefore, our findings do not question the role of surgery in lung cancer management. Rather, our results could be of interest when lung cancer is exposed to mechanical ventilation but not resected, such as during respiratory failure or major surgery without removal of the tumor. In this setting, mechanical priming of cancer cell could increase their invasiveness. However, the preclinical nature of our findings preclude their immediate translation to the clinical practice. Moreover, our clinical data is limited by the sample size and the retrospective nature of the analysis, so other hidden factors cannot be discarded. Therefore, it must be highlighted that we do not provide evidence that mechanical ventilation (either invasive or non-invasive) must be avoided in cancer patients. Rather, the impact of ventilation and our proposed therapies must be tested and validated in clinical studies.

In conclusion, we have shown that mechanical stimulation of cancer cells increases their invasiveness. This aggressive phenotype is dependent on intracellular cholesterol depletion, so interference with these pathways may limit cell migration in this setting. These mechanodependent pathways could be novel therapeutic targets that help to limit the metastatic spread of lung tumors and thus improve their outcome.

References

1. Orr AW, Helmke BP, Blackman BR, Schwartz MA. Mechanisms of mechanotransduction. *Dev Cell* 2006;10:11–20.
2. Wang N. Review of Cellular Mechanotransduction. *J Phys D Appl Phys* 2017;50:.
3. Gutierrez JA, Gonzalez RF, Dobbs LG. Mechanical distension modulates pulmonary alveolar epithelial phenotypic expression in vitro. *Am J Physiol* 1998;274:L196-202.
4. Edwards YS, Sutherland LM, Power JH, Nicholas TE, Murray AW. Cyclic stretch induces both apoptosis and secretion in rat alveolar type II cells. *FEBS Lett* 1999;448:127–130.
5. Wirtz HR, Dobbs LG. Calcium mobilization and exocytosis after one mechanical stretch of lung epithelial cells. *Science* 1990;250:1266–1269.
6. dos Santos CC, Han B, Andrade CF, Bai X, Uhlig S, Hubmayr R, Tsang M, Lodyga M, Keshavjee S, Slutsky AS, Liu M. DNA microarray analysis of gene expression in alveolar epithelial cells in response to TNFalpha, LPS, and cyclic stretch. *Physiol Genomics* 2004;19:331–342.
7. Slutsky AS, Ranieri VM. Ventilator-induced lung injury. *The New England journal of medicine* 2013;369:2126–36.
8. López-Alonso I, Blázquez-Prieto J, Amado-Rodríguez L, González-López A, Astudillo A, Sánchez M, Huidobro C, López-Martínez C, Dos Santos CC, Albaiceta GM. Preventing loss of mechanosensation by the nuclear membranes of alveolar cells reduces lung injury in mice during mechanical ventilation. *Sci Transl Med* 2018;10:eaam7598.
9. Blázquez-Prieto J, Huidobro C, López-Alonso I, Amado-Rodriguez L, Martín-Vicente P, López-Martínez C, Crespo I, Pantoja C, Fernandez-Marcos PJ, Serrano M, Sznajder

JI, Albaiceta GM. Activation of p21 limits acute lung injury and induces early senescence after acid aspiration and mechanical ventilation. *Transl Res* 2021;233:104–116.

10. Bade BC, Dela Cruz CS. Lung Cancer 2020: Epidemiology, Etiology, and Prevention. *Clin Chest Med* 2020;41:1–24.
11. Stella GM, Kolling S, Benvenuti S, Bortolotto C. Lung-Seeking Metastases. *Cancers (Basel)* 2019;11:.
12. Zhao X, Wen X, Wei W, Chen Y, Zhu J, Wang C. Clinical characteristics and prognoses of patients treated surgically for metastatic lung tumors. *Oncotarget* 2017;8:46491–46497.
13. Luo Y-H, Luo L, Wampfler JA, Wang Y, Liu D, Chen Y-M, Adjei AA, Midthun DE, Yang P. 5-year overall survival in patients with lung cancer eligible or ineligible for screening according to US Preventive Services Task Force criteria: a prospective, observational cohort study. *Lancet Oncol* 2019;20:1098–1108.
14. Mead J, Takishima T, Leith D. Stress distribution in lungs: a model of pulmonary elasticity. *J Appl Physiol* 1970;28:596–608.
15. Tse JM, Cheng G, Tyrrell JA, Wilcox-Adelman SA, Boucher Y, Jain RK, Munn LL. Mechanical compression drives cancer cells toward invasive phenotype. *Proc Natl Acad Sci U S A* 2012;109:911–916.
16. Polacheck WJ, German AE, Mammoto A, Ingber DE, Kamm RD. Mechanotransduction of fluid stresses governs 3D cell migration. *Proc Natl Acad Sci U S A* 2014;111:2447–2452.

17. Sanyour HJ, Li N, Rickel AP, Childs JD, Kinser CN, Hong Z. Membrane cholesterol and substrate stiffness co-ordinate to induce the remodelling of the cytoskeleton and the alteration in the biomechanics of vascular smooth muscle cells. *Cardiovasc Res* 2019;115:1369–1380.
18. Needham D, Nunn RS. Elastic deformation and failure of lipid bilayer membranes containing cholesterol. *Biophys J* 1990;58:997–1009.
19. Huang B, Song B-L, Xu C. Cholesterol metabolism in cancer: mechanisms and therapeutic opportunities. *Nat Metab* 2020;2:132–141.
20. López-Martínez C, Huidobro C, Albaiceta GM, López-Alonso I. Mechanical stretch modulates cell migration in the lungs. *Ann Transl Med* 2018;6:28.
21. Pickup MW, Mouw JK, Weaver VM. The extracellular matrix modulates the hallmarks of cancer. *EMBO Rep* 2014;15:1243–1253.
22. Gavara N, Sunyer R, Roca-Cusachs P, Farré R, Rotger M, Navajas D. Thrombin-induced contraction in alveolar epithelial cells probed by traction microscopy. *J Appl Physiol (1985)* 2006;101:512–520.
23. Charras G, Sahai E. Physical influences of the extracellular environment on cell migration. *Nat Rev Mol Cell Biol* 2014;15:813–824.
24. Fischer T, Hayn A, Mierke CT. Effect of Nuclear Stiffness on Cell Mechanics and Migration of Human Breast Cancer Cells. *Front Cell Dev Biol* 2020;8:393.
25. Krause M, Te Riet J, Wolf K. Probing the compressibility of tumor cell nuclei by combined atomic force-confocal microscopy. *Phys Biol* 2013;10:065002.
26. Urra H, Dufey E, Avril T, Chevet E, Hetz C. Endoplasmic Reticulum Stress and the Hallmarks of Cancer. *Trends Cancer* 2016;2:252–262.

27. Wang X, Xu W, Zhan P, Xu T, Jin J, Miu Y, Zhou Z, Zhu Q, Wan B, Xi G, Ye L, Liu Y, Gao J, Li H, Lv T, Song Y. Overexpression of geranylgeranyl diphosphate synthase contributes to tumour metastasis and correlates with poor prognosis of lung adenocarcinoma. *J Cell Mol Med* 2018;22:2177–2189.
28. Mullen PJ, Yu R, Longo J, Archer MC, Penn LZ. The interplay between cell signalling and the mevalonate pathway in cancer. *Nat Rev Cancer* 2016;16:718–731.
29. Suresh S. Biomechanics and biophysics of cancer cells. *Acta Biomater* 2007;3:413–438.
30. McKenney JM. Understanding PCSK9 and anti-PCSK9 therapies. *J Clin Lipidol* 2015;9:170–186.
31. Ferri N, Marchianò S, Tibolla G, Baetta R, Dhyani A, Ruscica M, Uboldi P, Catapano AL, Corsini A. PCSK9 knock-out mice are protected from neointimal formation in response to perivascular carotid collar placement. *Atherosclerosis* 2016;253:214–224.
32. Xu X, Cui Y, Cao L, Zhang Y, Yin Y, Hu X. PCSK9 regulates apoptosis in human lung adenocarcinoma A549 cells via endoplasmic reticulum stress and mitochondrial signaling pathways. *Exp Ther Med* 2017;13:1993–1999.
33. Sun X, Essalmani R, Day R, Khatib AM, Seidah NG, Prat A. Proprotein convertase subtilisin/kexin type 9 deficiency reduces melanoma metastasis in liver. *Neoplasia* 2012;14:1122–1131.
34. Momtazi-Borojeni AA, Nik ME, Jaafari MR, Banach M, Sahebkar A. Effects of immunisation against PCSK9 in mice bearing melanoma. *Arch Med Sci* 2020;16:189–199.

35. Liu X, Bao X, Hu M, Chang H, Jiao M, Cheng J, Xie L, Huang Q, Li F, Li C-Y. Inhibition of PCSK9 potentiates immune checkpoint therapy for cancer. *Nature* 2020;588:693–698.
36. Huang Y, Pan L, Helou K, Xia Q, Parris TZ, Li H, Xu B, Li H. Mechanical ventilation promotes lung metastasis in experimental 4T1 breast cancer lung-metastasized models. *Cancer Manag Res* 2018;10:545–555.
37. Sessler DI, Pei L, Huang Y, Fleischmann E, Marhofer P, Kurz A, Mayers DB, Meyer-Treschan TA, Grady M, Tan EY, Ayad S, Mascha EJ, Buggy DJ, Breast Cancer Recurrence Collaboration. Recurrence of breast cancer after regional or general anaesthesia: a randomised controlled trial. *Lancet* 2019;394:1807–1815.
38. Martinez-Garcia MA, Campos-Rodriguez F, Almendros I, Garcia-Rio F, Sanchez-de-la-Torre M, Farre R, Gozal D. Cancer and Sleep Apnea: Cutaneous Melanoma as a Case Study. *Am J Respir Crit Care Med* 2019;200:1345–1353.
39. Almendros I, Montserrat JM, Torres M, Dalmases M, Cabañas ML, Campos-Rodríguez F, Navajas D, Farré R. Intermittent hypoxia increases melanoma metastasis to the lung in a mouse model of sleep apnea. *Respir Physiol Neurobiol* 2013;186:303–307.
40. Cubillos-Zapata C, Almendros I, Díaz-García E, Toledano V, Casitas R, Galera R, López-Collazo E, Farre R, Gozal D, García-Rio F. Differential effect of intermittent hypoxia and sleep fragmentation on PD-1/PD-L1 upregulation. *Sleep* 2020;43:zsz285.
41. Cubillos-Zapata C, Martínez-García MÁ, Díaz-García E, Toledano V, Campos-Rodríguez F, Sánchez-de-la-Torre M, Nagore E, Martorell-Calatayud A, Hernández Blasco L, Pastor E, Abad-Capa J, Montserrat JM, Cabriada-Nuño V, Cano-Pumarega I, Corral-Peñafiel J, Arias E, Mediano O, Somoza-González M, Dalmau-Arias J,

Almendros I, Farré R, López-Collazo E, Gozal D, García-Río F, Spanish Sleep Network. Proangiogenic factor midkine is increased in melanoma patients with sleep apnea and induces tumor cell proliferation. *FASEB J* 2020;34:16179–16190.

Figure legends

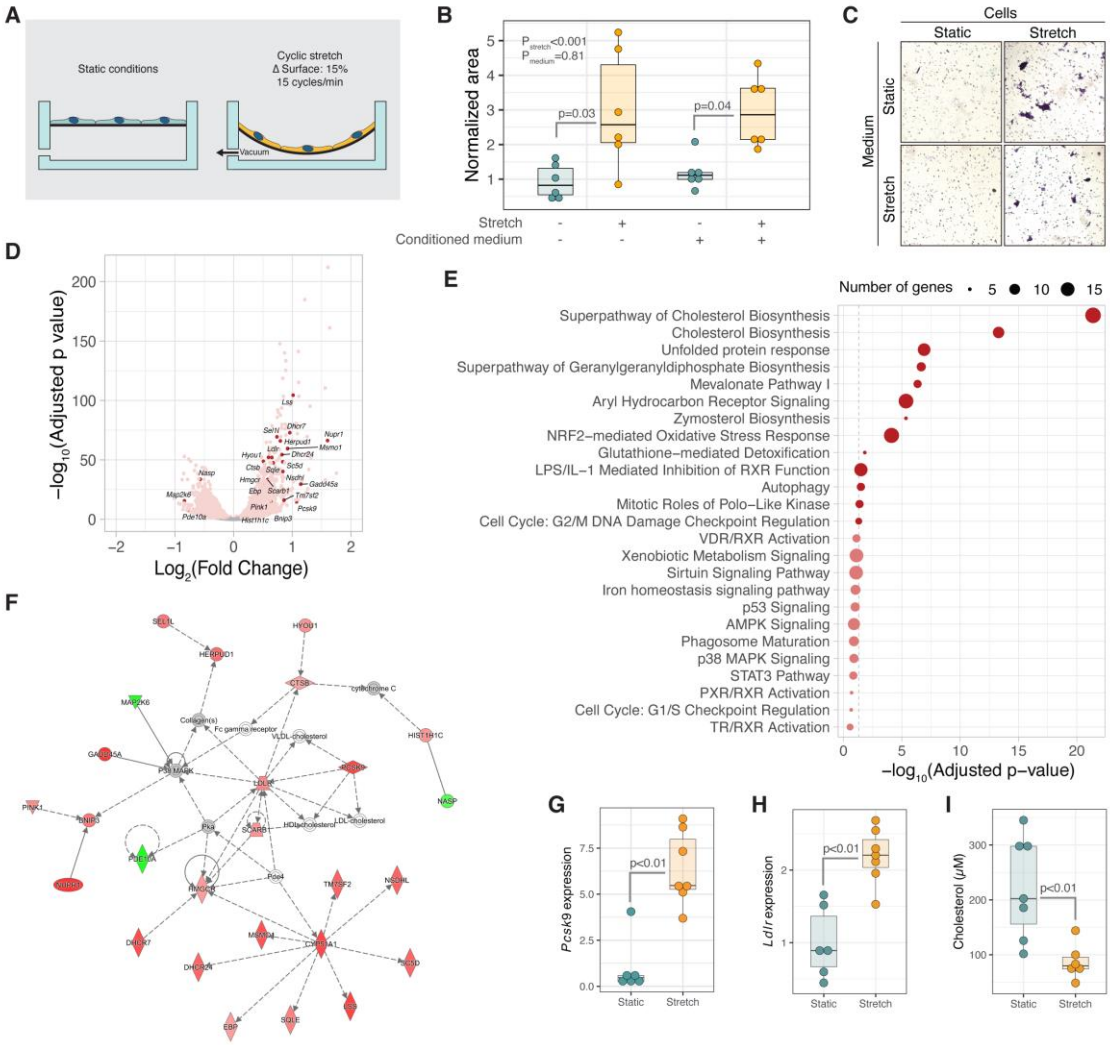

Figure 1. Changes in B16F10luc2 melanoma cells invasiveness in vitro after mechanical stretch.

a: Experimental model used: Cells were cultured in static conditions or submitted to cyclic stretch for 24 hours before invasion assays. **b**: Stretch increases the area covered by cells in the invasion chamber (n=6 per group), irrespective of the culture medium (see text for details). **c**: Representative images of the invasion chambers. **d**: Volcano plot showing changes in gene expression after mechanical stretch, with 5847 differentially expressed genes. Genes involved in cholesterol metabolism and included in the network depicted in panel 1f are highlighted. **e**: Overrepresented pathways in stretched cells,

according to Ingenuity Pathway Analysis software. Cholesterol-related pathways are among the most overrepresented routes. **f**: Gene network involved in cholesterol biosynthesis, showing genes upregulated by stretch (in red). **g-h**: Confirmation of the increase in *Pcsk9* (G) and *Ldlr* (H) expression after stretch, assessed by qPCR (n=6-7 per group). **i**: Mechanical stretch decreases intracellular cholesterol levels (n=6-7 per group). Boxplots represent the median (bold line), 1st and 3rd quartiles (hinges) and the largest/smallest values no further than 1.5 times the interquartile range from the corresponding hinge (whiskers). Values outside these whiskers can be considered outliers but were not excluded from analysis.

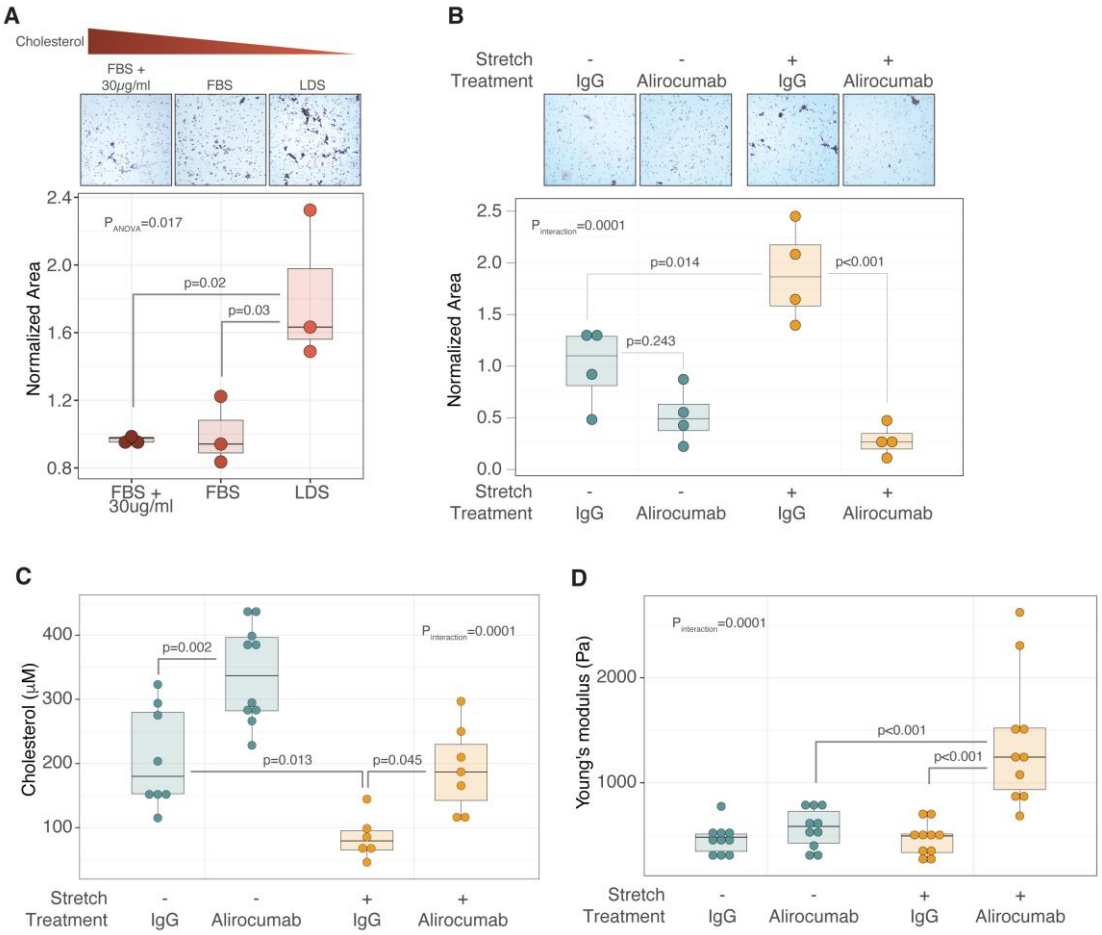

Figure 2. Modulation of B16F10luc2 invasiveness by cholesterol manipulation.

a: Cells cultured in lipid-depleted medium show an increase in invasiveness compared to cells cultured in standard conditions or supplemented with cholesterol (n=3 per group). FBS: Fetal bovine serum; LDS: Lipid depleted serum. **b**: Alirocumab, a monoclonal anti-PCSK9 neutralizing antibody, attenuates the increase in invasiveness caused by stretch (n=4 per group). **c**: Alirocumab increases intracellular cholesterol concentrations (n=6-10 per group). **d**: Alirocumab specifically increases cell stiffness (measured using atomic force microscopy) after mechanical stretch (n=10 per group). Boxplots represent the median (bold line), 1st and 3rd quartiles (hinges) and the largest/smallest values no further than 1.5 times the interquartile range from the

corresponding hinge (whiskers). Values outside these whiskers can be considered outliers but were not excluded from analysis.

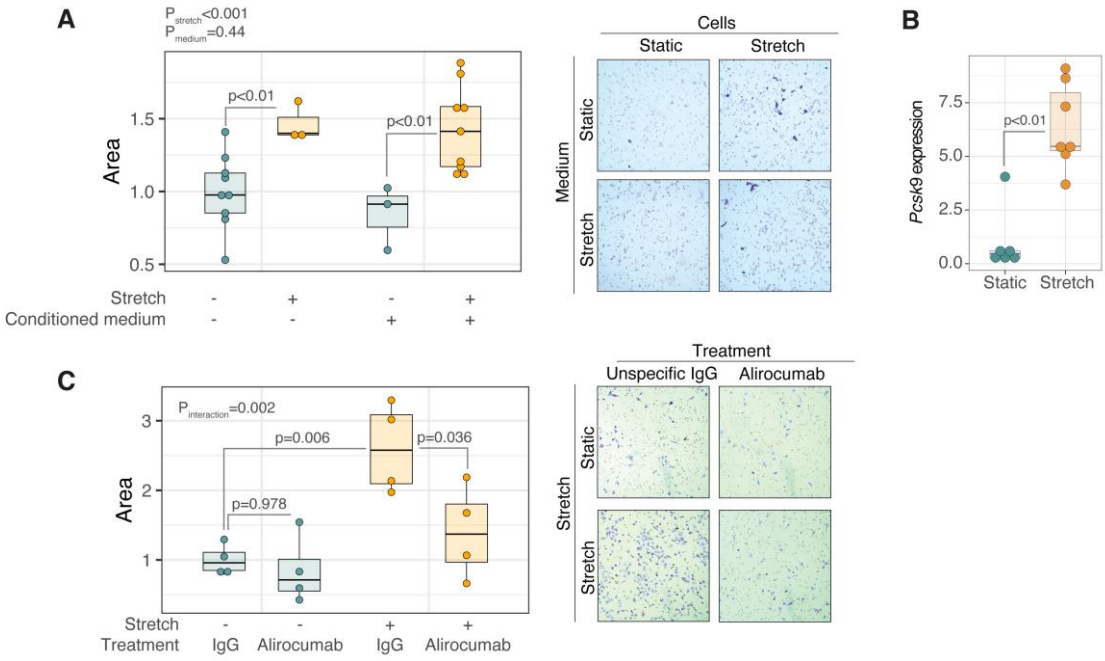

Figure 3. Validation of findings in A549 human lung adenocarcinoma cells. a: Mechanical stretch increased invasiveness of A549 cells (n=3-9 per group). **b:** Stretch-induced changes in PCSK9 expression (n=6-7 per group). **c:** As in murine melanoma cells, PCSK9 inhibition using alirocumab decreases invasion (n=4 per group). Boxplots represent the median (bold line), 1st and 3rd quartiles (hinges) and the largest/smallest values no further than 1.5 times the interquartile range from the corresponding hinge (whiskers). Values outside these whiskers can be considered outliers but were not excluded from analysis.

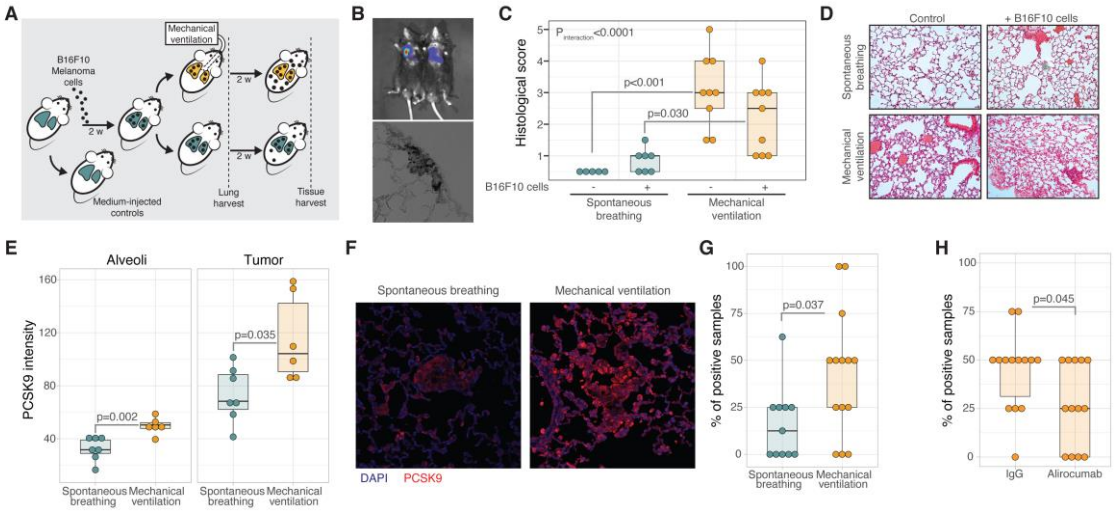

Figure 4. Effects of mechanical ventilation in an animal model of lung melanoma implants.

a: Experimental model. Mice were inoculated with B16F10luc2 cells, so that lung implants can be detected after 2 weeks. After this time, mice were randomized to receive mechanical ventilation or maintain spontaneous breathing, and followed for 2 additional weeks After this time, animals were sacrificed, brain and kidneys harvested and the presence of melanoma cells assessed by qPCR. Medium-injected mice were used as controls. **b**: Lung implants after two weeks, detected by chemoluminiscence (up) and in histological sections (down). **c**: Increases in lung injury immediately after mechanical ventilation in mice with and without melanoma implants (n=5-9 per group). **d**: Representative lung histological sections after mechanical ventilation in all the experimental groups. **e**: Quantification of PCSK9 in lungs after mechanical ventilation in alveoli and tumor implants (n=6-7 per group). Mechanical ventilation increased PCSK9 fluorescence intensity. **f**: Representative images of lung sections immunostained with an antibody against PCSK9 in all the experimental groups. **g**: Mechanical ventilation increases the percentage of brain and kidney samples with positive detection of *Luc2*

expression, suggestive of micrometastases (n=11-14 mice per group). **h**: Mice with lung melanoma implants and treated with alirocumab show a lower percentage of brain and kidney Luc2-positive samples than those treated with unspecific IgG (n=13-14 mice per group). Boxplots represent the median (bold line), 1st and 3rd quartiles (hinges) and the largest/smallest values no further than 1.5 times the interquartile range from the corresponding hinge (whiskers). Values outside these whiskers can be considered outliers but were not excluded from analysis.

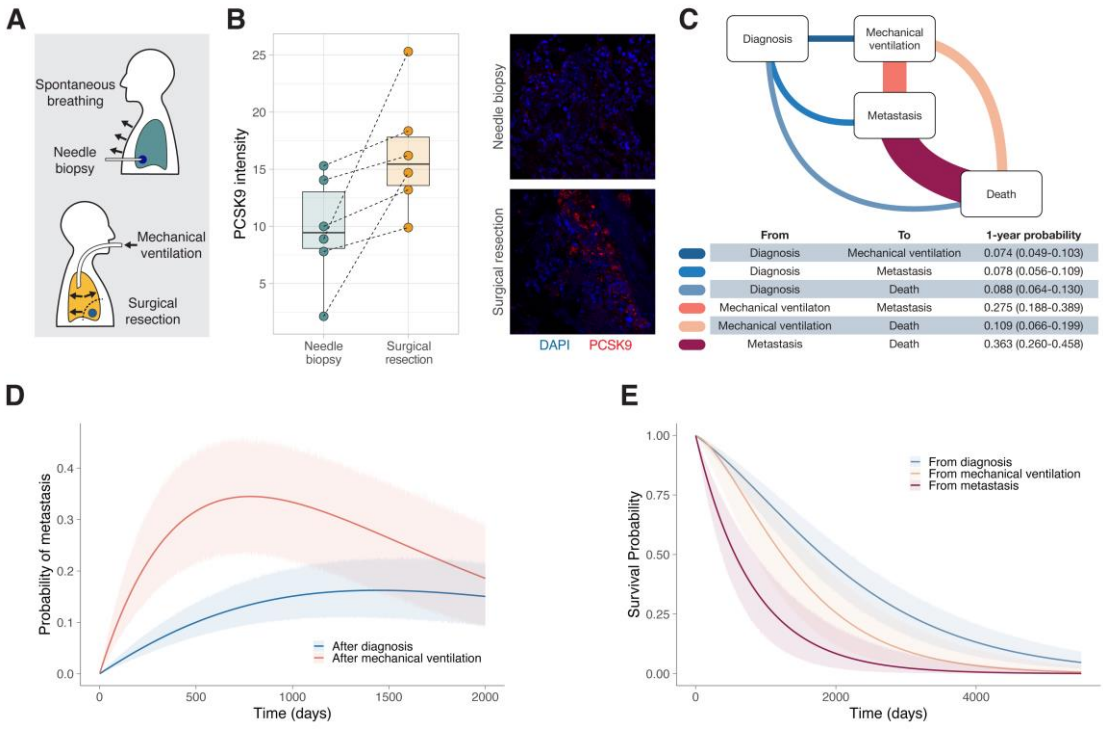

Figure 5. Effects of mechanical ventilation on patients with lung cancer.

a: Experimental model: A group of 6 lung adenocarcinomas that were biopsied in patients (under spontaneous breathing) and later surgically removed (under mechanical ventilation) were studied. **b**: PCSK9 fluorescence intensity in paired samples obtained in both ventilatory conditions, and representative immunohistochemical sections. PCSK9 abundance increased in all the tumors after mechanical ventilation and surgical resection. Boxplots represent the median (bold line), 1st and 3rd quartiles (hinges) and the largest/smallest values no further than 1.5 times the interquartile range from the corresponding hinge (whiskers). Values outside these whiskers can be considered outliers, but were not excluded from analysis. Dotted lines connect samples from the same patient under different conditions. **c**: Clinical model. Twenty-eight patients with localized lung cancer that received mechanical ventilation for any cause other than surgical resection of the tumor were matched to 58 patients that were not ventilated. A

multi-state Markov model including mechanical ventilation, development of metastasis and death as possible states was used to predict transition probabilities, as shown in the table. Line width in the figure is proportional to these probabilities. **d-e**: Probability of metastasis after diagnosis or after mechanical ventilation (**d**) and predicted survival from each state (**e**). Mechanical ventilation increased the risk of metastasis (HR 4.91, 95% confidence interval 2.68-9.03) and both mechanical ventilation (HR 1.50, 95% confidence interval 1.44-1.58) and metastases (HR 3.13, 95% confidence interval 2.95-3.33) worsened the outcome.

Mechanical ventilation promotes lung tumor spread by modulation of cholesterol cell content

Inés López-Alonso, Cecilia López-Martínez, Paula Martín-Vicente, Laura Amado-Rodríguez, Adrián González-López, Juan Mayordomo-Colunga, Cecilia del Busto, Marina Bernal, Irene Crespo, Aurora Astudillo, Miguel Arias-Guillén, Antonio Fueyo, Isaac Almendros, Jorge Otero, Héctor Sanz-Fraile, Ramón Farré, Guillermo M Albaiceta.

Online supplement

Detailed methods

Study overview

To test the hypothesis that the cyclic stretch of mechanical ventilation increases cancer cell aggressiveness, a combination of cell and animal experiments and clinical observations were performed. Cancer cell lines were cultured in static conditions or under cyclic stretch, and their invasiveness assessed. The transcriptomes of these cells were compared to identify the molecular pathways responsible for the phenotypic changes, that were confirmed by pharmacological interference experiments. Mice harbouring lung melanoma implants were submitted to mechanical ventilation to study the *in vivo* effects of mechanical stretch and its impact on the systemic spread of these tumours. Finally, in a cohort of lung cancer patients that received mechanical ventilation, the incidence of distant metastases was compared with a matched group of non-ventilated patients.

Cell culture and invasiveness measurements

Mouse melanoma B16F10luc2 cells (with constitutive expression of firefly luciferase) and human lung adenocarcinoma A549 cells were cultured in elastic plates (Bioflex culture plates, Flexcell int.) at a density of $2x10^5$, in DMEM + 10% FBS and standard culture conditions (37°C, 21% O_2, 5% CO_2). After 24 h cells were exposed to cyclic stretch (15% elongation, 15 cycles/min, 1:1 stretch:relaxation ratio) for 24 h. Non-stretched cells, cultured in the same plates were used as control. Afterwards, cells were dissociated using EDTA (1 mM, 10 min incubation) to minimize proteolysis and cell membrane damage (1). Removal of cells was confirmed by optical microscopy. For quantitative PCR and RNAseq analysis, cells were homogenized with TRIzol® (Invitrogen).

In separate experiments, cell invasiveness was assessed using 8 µm Matrigel transwells (Corning). Fifty thousand stretched cells and their respective controls were dissociated as previously described and seeded in the upper chamber with culture media, and DMEM + 10% FBS added in the bottom chamber. In order to study the possible effect of paracrine factors, additional wells were seeded with static or stretched cells in combination with supernatant from other group of the same experiment. Therefore, 4 possible combinations (static cells + static supernatant; static cells + stretched supernatant; stretched cells + static supernatant; stretched cells + stretched supernatant) were studied. After 24 h, transwells were fixed and dyed with 0,1% crystal violet in 100% methanol, and the Matrigel layer removed. An image of the membrane was taken with an optical microscope (5X magnification) and the area covered by migrated cells was quantified using ImageJ software. Additionally, B16F10 cells were stretched and invasiveness assayed as described using culture conditions with different CO_2 concentrations (5% and 20%).

RNA sequencing

RNA from B16F10luc2 cells in static or stretched conditions was extracted with the RNeasy Mini Kit (Qiagen). RNA quality verification, library construction and sequencing were performed using a standard pipeline (BGI Genomics). Samples were processed for quality check and removal of adapters. Clean reads are available at Gene Expression Omnibus repository (accession number GSE168499, https://www.ncbi.nlm.nih.gov/geo/query/acc.cgi?acc=GSE168499). Read counts were calculated by pseudoalignment to the mm10 mouse reference transcriptome using the Salmon v1.4 software **(2)**. Differential expression analysis was performed using the

DESeq2 library for the R statistical software (3). P-values were adjusted using the Benjamini-Hochberg method for a false discovery rate of 5%. Genes with a fold change higher than 0.5 log were introduced in the Ingenuity Pathway Analysis software (Quiagen) to identify overrepresented pathways.

Alirocumab treatment in cells

During *in vitro* experiments, stretched cells were treated with alirocumab 7.5 µg/ml (Praluent, Sanofi) or IgG control 7.5 µg/ml (Invitrogen) added to the culture medium 3 days prior to mechanical stress, and invasiveness was assessed as previously described.

Cholesterol measurements

Intracellular cholesterol was quantified using the *Total Cholesterol Kit* (Cell Biolabs). Cells were homogenized in a 7:11:0.1 solution of chloroform:isopropanol:NP-40. Samples were centrifuged and the organic phase left to evaporate at 50°C. The remaining lipidic pellet was resuspended in the reaction buffer, incubated 45 min at 37°C and absorbance measured in the 540-570 nm range.

In vitro cholesterol treatment

B16F10luc2 or A549 cells were cultured in plastic plates and treated with either cholesterol supplemented medium (30 µg/ml cholesterol (Sigma-Aldrich) in DMEM + 10% FBS), cholesterol-depleted medium (DMEM + 10% Lipid Depleted Serum (VWR) or control medium (DMEM + 10% FBS) for 72h. Then, invasiveness potential was assessed using Matrigel chambers as previously described.

Atomic Force Microscopy

B16F10luc2 cells were cultured in Bioflex culture plates and treated with alirocumab or IgG control as previously described. After being subjected to stretch or static condition, the nuclei of the cells were stained using NucBlue (ThermoFisher). Elastic modulus of cells was measured by Atomic Force Microscopy (AFM): plates were placed in a custom-built AFM mounted on an inverted optical microscope (Nikon TE2000) with epifluorescence, and equipped with a V-shaped silicon nitride cantilever with a nominal spring constant of 0.01N/m ended with a silicon dioxide spherical tip of 5 microns in diameter (Novascan Technologies). The elastic modulus of the cell nucleus was computed from the average of five force-displacement curves (at a speed of 1 µm/s) by adjusting the Hertz model at 500 nm indentation depth as previously described **(4)**. To avoid local effects, a maximum of 2 cells from the same field of view were measured, and never contiguous with each other. Stiffness of each cell nucleus was characterized as the average from the different curves recorded in the sample.

Animal models

All experiments were approved and performed according to guidelines set out by the Animal Research Committee of the University of Oviedo, Spain (protocol approval numbers 19-INV-2012 and PROAE 18/2020). Animals were maintained in specific pathogen-free conditions with 12-hour light/dark cycles and *ad libitum* access to water and food.

Mice were anesthetized by intraperitoneal injection of a mixture of ketamine and xylazine. Then, 15000 B16F10luc2 cells in 100 µl of cell culture medium or vehicle were injected via jugular vein. Development of melanoma implants was monitored by

bioluminescence after injection of luciferine (45 mM, 200 µl intraperitoneal) in an *in vivo* optical imaging equipment (IVIS, PerkinElmer) every 5 days. Fifteen days after the injection, mice were randomized to spontaneous breathing or intubation and connection to a mechanical ventilator (Evita 2 Dura-Neoflow, Drager) for 2 hours in pressure-controlled mode to keep driving pressure constant (peak inspiratory pressure 15 cmH_2O, PEEP: 2 cmH_2O, 100 breaths/min) under anesthesia as previously described (5). In preliminary experiments, these settings result in tidal volumes of 10 ml/Kg at the start of ventilation in both groups and cause a moderate lung damage but ensure post-ventilation survival. A second randomization was performed after ventilation, and mice assigned to immediate sacrifice or follow up.

For the first case, animals were sacrificed by exsanguination and lungs, kidney and brain were immediately removed. The right bronchus was tied and the right lung was frozen at -80°C for subsequent analysis. The left lung was fixated with intratracheal 4% formaldehyde and immersed in the same fixative for histological analysis.

Mice assigned to follow-up were treated with atropine (0.05 mg/kg, intraperitoneally injected) and disconnected from the ventilator. When awake, mice were extubated and left to recover under a heating lamp. Fifteen days after ventilation, animals were anesthetized, sacrificed by exsanguination and lungs, brain and kidney, were harvested for histological and biochemical analysis.

Two additional animal series were performed. To discard the role of inflammation in the observed results, mice were injected with melanoma cells as previously described and, after 15 days, treated with lipopolysaccharide (LPS from *E. coli*, 15 mg/kg; serotype O55:B5, Sigma-Aldrich), followed up for 15 additional days and sacrificed as described above. In an additional series aimed to discard the role of the systemic response to

ventilation, mice were anesthetized by intraperitoneal injection of a mixture of ketamine and xylazine and 15000 B16F10luc2 cells were injected by spleen puncture. After the injection, a splenectomy was performed. This procedure resulted in liver melanoma implants, macroscopically visible two weeks after injection. Fifteen days after the procedure, mice were intubated, ventilated and followed up for 15 additional days as described above.

Alirocumab treatment in the animal model

Mice harboring lung melanoma implants were randomized to receive treatment with Alirocumab (Praluent, Sanofi) or unspecific IgG (Invitrogen). Three 10 mg/kg doses of either drug were administered (7 and 2 days before and 1 day after ventilation). This regime constitute the most studied alirocumab dose in mice (6, 7), with an additional dose before ventilation aimed to achieve high PCSK9 inhibition rates after mechanical ventilation. In this series, animals were mechanically ventilated and, after 15 days, anesthetized and organs harvested as described. Humane endpoints were considered in all animal models: euthanasia was performed if tumoral mass covered more than 75% of the targeted organ, or if rapid weight loss, inability to ambulate, labored respiration or evident signs of pain were observed.

Histological and immunofluorescence studies

After fixation, the left lung was embedded in paraffin, and three slices, with a minimal separation of 1 mm between them, were stained with hematoxylin-eosin. A pathologist blinded to experimental conditions evaluated the severity and extent of lung injury using a previously defined score (8).

For immunofluorescence studies, slices were deparaffinated and antigens retrieved in citrate buffer 0.1M (pH 9). The autofluorescence of the tissue was diminished using a Sudan Black saturated solution for 30 min. Afterwards, sections were permeabilized with 0.1% Triton X-100 in PBS for 15 min, blocked with 1% BSA in PBS and incubated overnight at 4°C with a primary antibody against PCSK9 (ab95478, Abcam). The next day the slices were incubated with the corresponding secondary fluorescent antibody (anti-rabbit AlexaFluor-594, Thermo Fisher Scientific) at room temperature for 45 min. Staining with phalloidin-iFluor 594 (ab176757, Abcam) and Deoxyribonuclease I Alexa Fluor 488 conjugate (D12371, Invitrogen) were used for F-actin and G-actin detection respectively. Brain right hemispheres from qPCR-positive and qPCR-negative animals were fixed, embedded in paraffin and serial coronal section were cut and immunostained with an antibody against GP100 (ab137078, Abcam), a specific melanoma marker.

All slides were mounted with SlowFade Diamond Mountant with DAPI (Invitrogen) For nuclear visualization. Images were taken using a confocal microscopy (Leica SP8) at 40x and 63x. Fluorescence intensity was quantified using ImageJ software (NIH). Acquisition parameters were kept constant for all the images. Tumor areas were manually delimitated using a composite image including fluorescence and brightfield channels. Fluorescence mean intensity was quantified in the selected areas after background correction using ImageJ built-in tools.

Quantitative PCR

Cell cultures and tissue samples (2 mm x 2 mm) were homogenized with TRIzol® (Invitrogen) and RNA precipitated overnight with isopropanol at - 20°C. After 24 h, samples were washed with ethanol and the collected RNA resuspended in RNAse-free

water and quantified in an Epoch Microplate Spectrophotometer (BioTek, Agilent). One µg of total RNA was retrotranscribed into cDNA using an RT-PCR kit (High-capacity cDNA rt Kit, Applied Biosystems). Quantitative PCRs were carried out in triplicate for each sample. Tissue metastases were detected by *Luc2* amplification using 100 ng of cDNA. Samples in which the gene was amplified were considered as positive for metastasis (9). For each animal, a metastatic score was calculated as the mean of positive samples for *Luc2* gene in both kidney and brain.

Expression of *Pcsk9* and *Gapdh* in animal tissues and *PCSK9* and *GAPDH* in human cells was quantified using 5 ng of cDNA per well. Sybr-green Power up (Thermo Fisher Scientific) and 10 µM of the corresponding primers (Supplementary Table 1) were used in all the experiments. The relative expression of each gene was calculated as $2^{-\Delta CT(\text{gene of interest}) - \Delta CT(\text{housekeeping gene})}$.

Patients

A retrospective, observational study was designed to test the hypothesis that mechanical ventilation could promote the systemic spread of lung cancers. The protocol was approved by the regional ethics committee on clinical research (Comité de Ética de la Investigación del Principado de Asturias, ref. 119/18). Due to the observational nature of the study, informed consent was waived.

First, six pairs of lung adenocarcinoma samples obtained by large-bore needle aspiration (under spontaneous breathing) and during surgical resection (after mechanical ventilation) available at the Hospital Universitario Central de Asturias (Oviedo, Spain) Biobank. Histological sections of these samples were immunostained using an anti-PCSK9 antibody and the fuoresecence images obtained and quantified as previously described.

Second, all patients with a diagnosis of primary lung cancer without distant metastases who received mechanical ventilation for any reason except anesthesia for lung cancer resection, from July-2014 to November-2019, at Hospital Universitario Central de Asturias were considered cases. Two control patients (with non-metastatic, primary lung cancer who did not receive mechanical ventilation), matched by sex, age and tumor stage, obtained from hospital database, were included per each case. Clinical data including demographical variables, smoking history, treatments received for lung cancer, dates of mechanical ventilation, diagnosis of first distant metastases and last follow up, and survival status were collected.

Statistical analysis

Comparisons between groups were done using ANOVA, Wilcoxon or Fisher tests (for more than two groups, continuous and categorical variables respectively) and two-sided p-values calculated.

To characterize the effect of mechanical ventilation on the development of metastases in patients, a multi-state Markov model was defined using the msm package for R (10). By assuming that future evolution only depends on the current state, and not on the previous trajectory, this model takes into account the time-dependent effect of mechanical ventilation and the existence of a competing risk between death and development of metastases. The matrix of transition probabilities between the different states of the model and survival curves for each state were calculated. Hazard ratios between survival curves or state transition probabilities (with their 95% confidence intervals) were calculated using a bootstrap algorithm. All the calculations were performed using the statistical software R (version 4.0.3).

Supplementary results

Supplementary Figure 1: Markers of stretch in cultured cells. a: Cultured cells submitted to mechanical stretch showing an increase in fibrillar actin (F-actin) over its globular, monomeric form (G-Actin). **b (next page):** Quantification of F-actin/G-actin ratios.

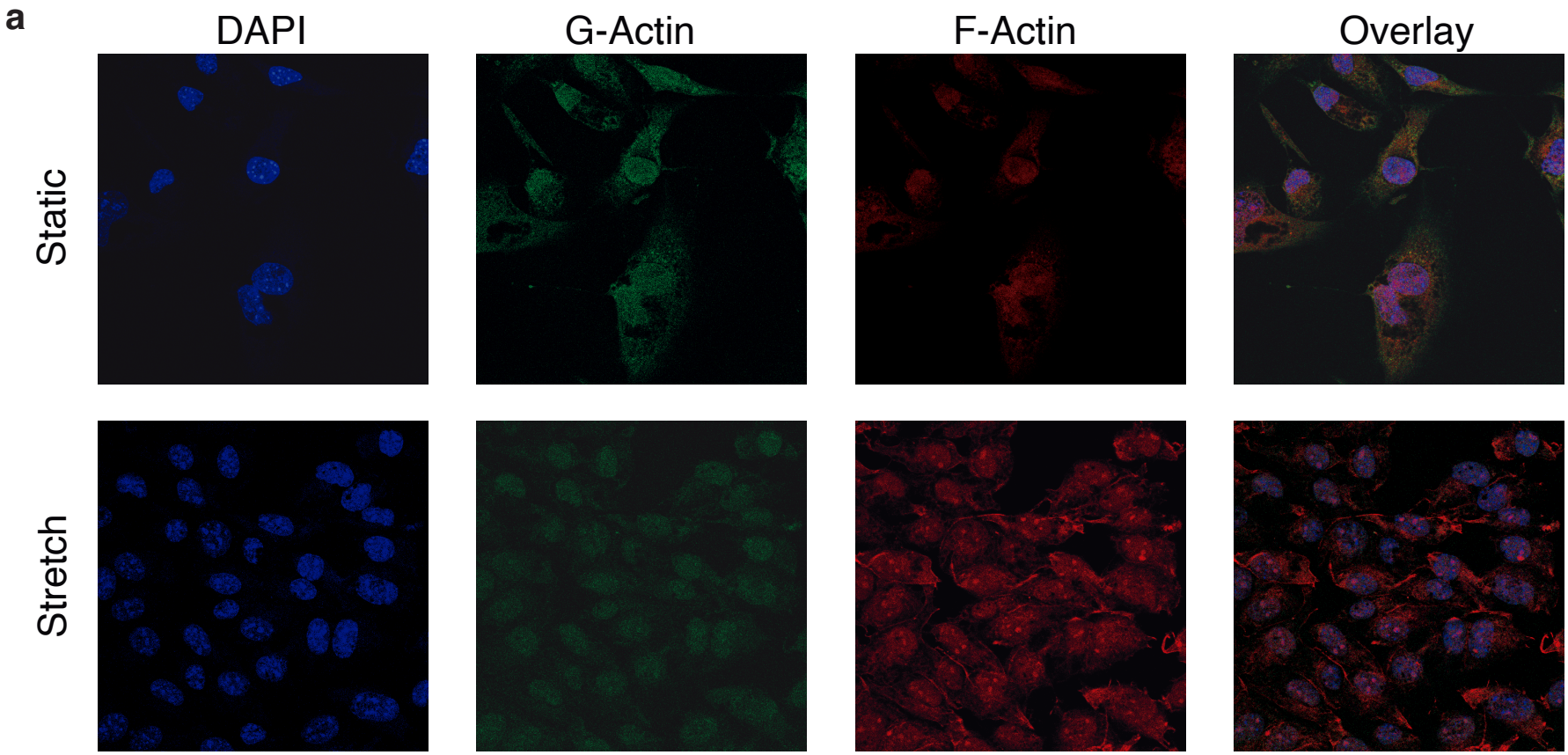

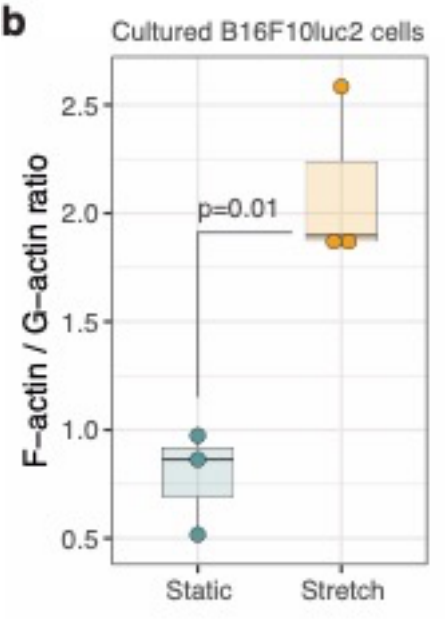
b
Cultured B16F10luc2 cells
F−actin / G−actin ratio
2.5
2.0
1.5
1.0
0.5
p=0.01
Static
Stretch

Supplementary Figure 2: Markers of stretch in ventilated animals. a: Mechanical ventilation increased fibrillar actin (F-actin), in both normal tissue and lungs with melanoma implants. b: Quantification of F-actin/G-actin ratios.

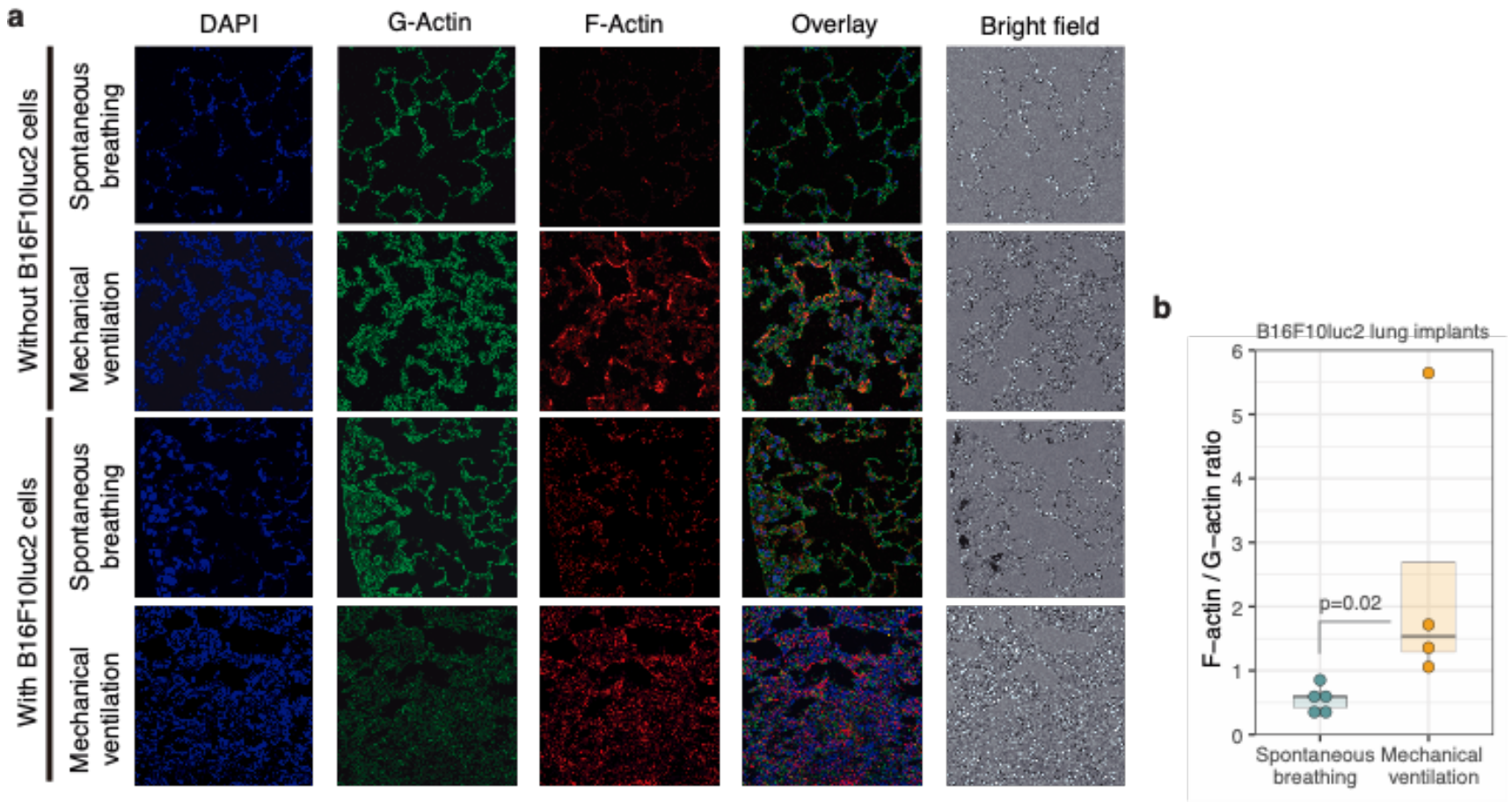

Supplementary Figure 3: Identification of brain metastases. To confirm the presence of metastatic B16F10luc2 cells, coronal serial slices of right hemispheres from animals with negative and positive qPCR for luciferase-2 (n=3 per group) were stained with antibodies against the melanoma marker GP100. Positive cells were identified only in animals with a positive qPCR. Panels show representative sections.

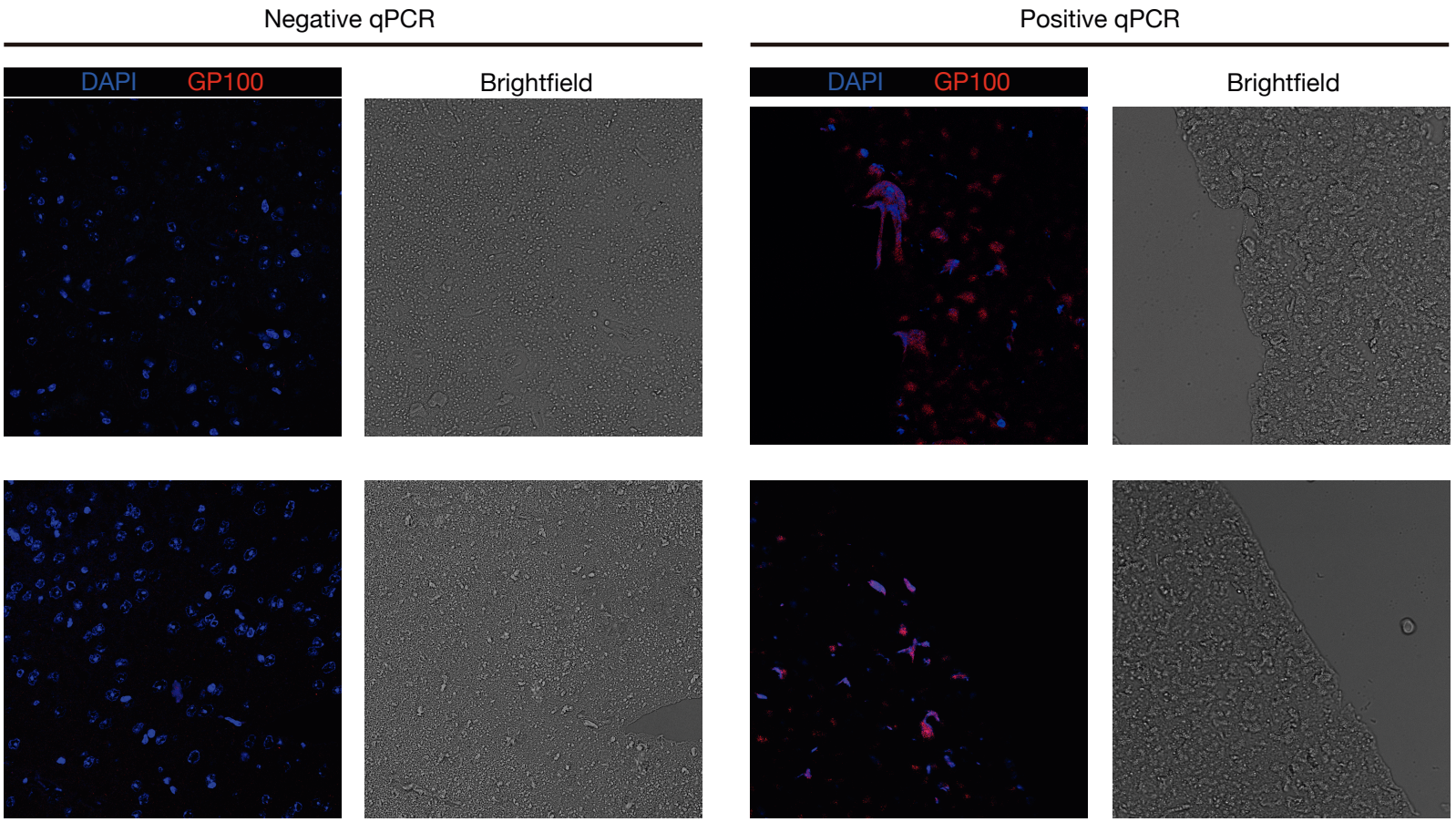

Supplementary Figure 4: Alternative models of cancer and lung injury. Incidence of brain and kidney metastasis in mice with liver melanoma implants and submitted to mechanical ventilation (**a**) and in mice with lung melanoma implants treated with LPS (**b**).

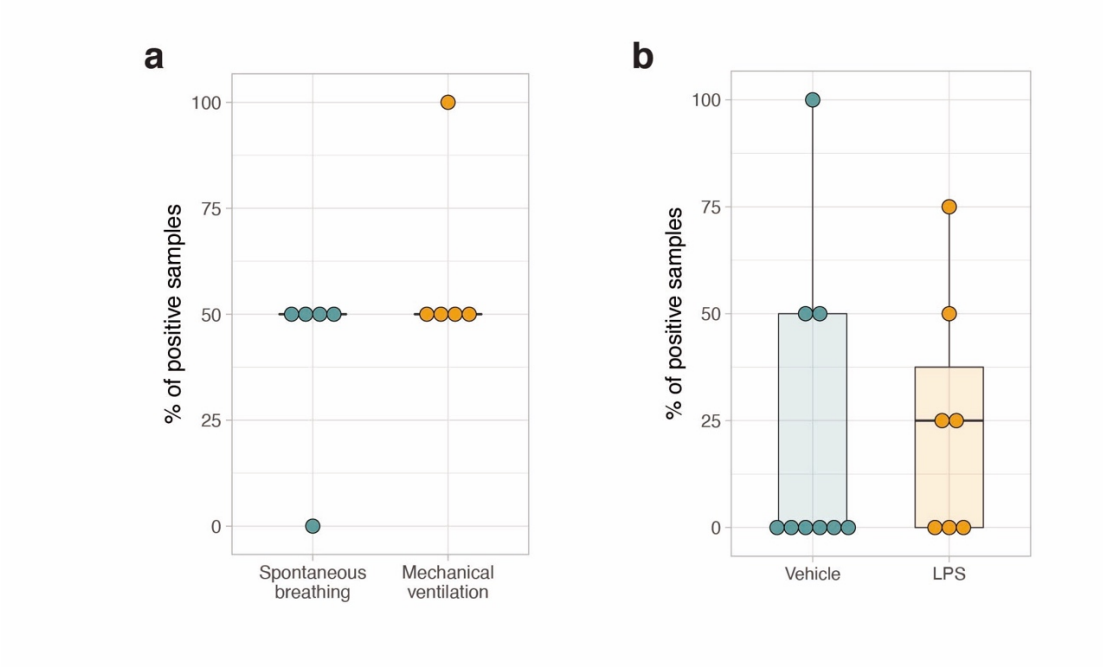

Supplementary figure 5. Effects of CO_2 on invasiveness of B16F10luc melanoma cells.

Increasing CO_2 concentration from 5% to 20% promoted cell invasiveness in Matrigel chambers.

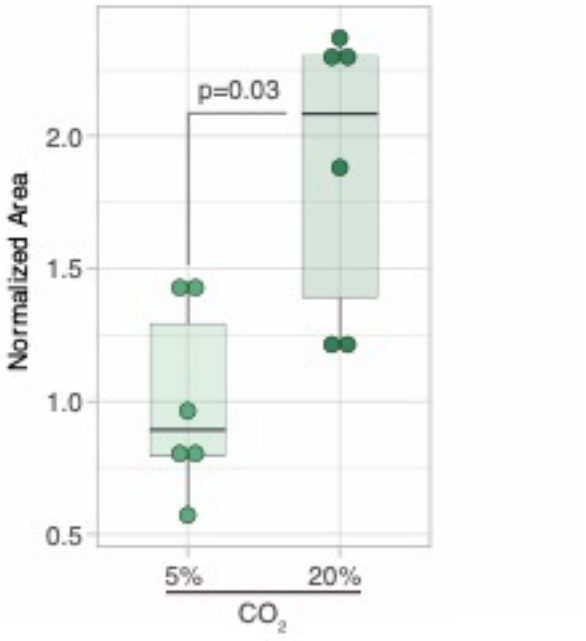

Supplementary Table 1. Primers used for qPCR.

Gene	Forward	Reverse
GAPDH	5'-TCGGAGTCAACGGATTTGGTCGT-3'	5'-TGCCATGGGTGGAATCATATTGGA-3'
Gapdh	5'-GTGCAGTGCCAGCCTCGTCC-3'	5'-GCCACTGCAAATGGCAGCCC-3'
PCSK9	5'-GCTGAGCTGCTCCAGTTTCT-3'	5'-AATGGCGTAGACACCCTCAC-3'
Pcsk9	5'-GAGATTATGAAGAGCTGATGC-3'	5'-GTTTGTTCAATCTGTAGCCTC-3'
Luc2	5'-AAACGCTTCCACCTACCAGG-3'	5'-CCTTAGCCTCGAAGAAGGGC-3'

Supplementary table 2. Clinical data from lung cancer patients that received mechanical ventilation by any cause other than lung cancer surgery, and their controls. *Tumor stage was analyzed only for non-small cell lung cancer. All small cell lung cancer cases were in a limited stage. IQR: Interquartile range.

	Non-ventilated (N=58)	Ventilated (N=28)	P value
Age (median, IQR)	70 (63 - 73)	66 (61 - 71)	0.162
Sexo			0.066
Female	9	10	
Male	49	18	
Comorbidities			
COPD	21	7	0.427
Cardiac disease	14	5	0.704
Vascular disease	8	6	0.581
Neurovascular disease	4	6	0.107
Immunosuppression	3	0	0.541
Sleep apnea	2	1	1.000
Chronic renal disease	3	1	1.000
Diabetes	13	4	0.550
Tumor stage*			0.15
I	10	8	
II	15	3	
III	19	13	
Cancer type			0.06
Squamous	27	9	
Adenocarcinoma	16	15	
Small cell	15	4	
Smoking history			0.982
Past	34	16	
Active	19	9	
Non-smoker	5	2	
Treatments			
Radiotherapy	40	16	0.403
Chemotherapy	27	18	0.189
Surgery	16	10	0.604

Supplementary references

1. Beers J, Gulbranson DR, George N, Siniscalchi LI, Jones J, Thomson JA, Chen G. Passaging and colony expansion of human pluripotent stem cells by enzyme-free dissociation in chemically defined culture conditions. *Nat Protoc* 2012;7:2029–2040.
2. Patro R, Duggal G, Love MI, Irizarry RA, Kingsford C. Salmon provides fast and bias-aware quantification of transcript expression. *Nat Methods* 2017;14:417–419.
3. Love MI, Huber W, Anders S. Moderated estimation of fold change and dispersion for RNA-seq data with DESeq2. *Genome Biol* 2014;15:550.
4. Alcaraz J, Otero J, Jorba I, Navajas D. Bidirectional mechanobiology between cells and their local extracellular matrix probed by atomic force microscopy. *Semin Cell Dev Biol* 2018;73:71–81.
5. Albaiceta GM, Gutierrez-Fernandez A, Garcia-Prieto E, Puente XS, Parra D, Astudillo A, Campestre C, Cabrera S, Gonzalez-Lopez A, Fueyo A, Taboada F, Lopez-Otin C. Absence or inhibition of matrix metalloproteinase-8 decreases ventilator-induced lung injury. *Am J Respir Cell Mol Biol* 2010;43:555–63.
6. Kühnast S, van der Hoorn JWA, Pieterman EJ, van den Hoek AM, Sasiela WJ, Gusarova V, Peyman A, Schäfer H-L, Schwahn U, Jukema JW, Princen HMG. Alirocumab inhibits atherosclerosis, improves the plaque morphology, and enhances the effects of a statin. *J Lipid Res* 2014;55:2103–2112.
7. Pouwer MG, Pieterman EJ, Worms N, Keijzer N, Jukema JW, Gromada J, Gusarova V, Princen HMG. Alirocumab, evinacumab, and atorvastatin triple therapy regresses plaque lesions and improves lesion composition in mice. *J Lipid Res* 2020;61:365–375.
8. Blazquez-Prieto J, Lopez-Alonso I, Amado-Rodriguez L, Batalla-Solis E, Gonzalez-Lopez A, Albaiceta GM. Exposure to mechanical ventilation promotes tolerance to ventilator-induced lung injury by Ccl3 downregulation. *Am J Physiol Lung Cell Mol Physiol* 2015;309:L847-56.
9. Deng W, McLaughlin SL, Klinke DJ. Quantifying spontaneous metastasis in a syngeneic mouse melanoma model using real time PCR. *The Analyst* 2017;142:2945–2953.
10. Jackson C. Multi-State Models for Panel Data: The msm Package for R. *J Stat Softw Artic* 2011;38:1–28.